Reactive and Functional Polymers 130 (2018) 111–117

Contents lists available at ScienceDirect

Reactive and Functional Polymers

journal homepage: www.elsevier.com/locate/react

Semiflexible ring polymers in dilute solutions

Daichi Ida*

Department of Polymer Chemistry, Kyoto University, Katsura, Kyoto 615-8510, Japan

ARTICLE INFO

Keyword:
Intrinsic viscosity
Mean-square radius of gyration
Scattering function
Second virial coefficient
Semiflexible ring polymers

ABSTRACT

Our recent theoretical and/or Monte Carlo results for dilute solution properties of semiflexible ring polymers on the basis of the wormlike ring model are briefly summarized. The behavior of the mean-square radius of gyration $\langle S^2 \rangle$, intrinsic viscosity $[\eta]$, scattering function $P(k)$ with k the magnitude of the scattering vector, and second virial coefficient $A_{2,\Theta}$ at the Θ state is examined as a function of the reduced contour length λL, where λ^{-1} and L are the stiffness parameter and contour length of the wormlike ring, respectively. Effects of the topological constraints on $\langle S^2 \rangle$, $[\eta]$, $P(k)$, and $A_{2,\Theta}$ of semiflexible rings are also examined by comparing the results for the wormlike rings without the topological constraints with those for the wormlike ring of the trivial or trefoil knot.

1. Introduction

Dilute solution properties of ring polymers have long been investigated mainly for *flexible* ring polymers, such as polystyrene (PS), polydimethylsiloxane, and so on, using with the Gaussian ring theories for analysis of experimental data [1, 2, 3]. The Gaussian ring theories are valid only for ring polymers of very large molecular weight M (strictly speaking, in the limit of $M \to \infty$), and then, can never be used for *semiflexible* ring polymers, such as circular deoxyribonucleic acids [4], cyclic amylose tris(alkylcarbamate)'s (cATACs) reported recently by Terao et al. [5, 6], and so on. Theoretical and/or computational studies on the basis of a proper model for semiflexible rings are then desired.

As is well known, the dilute solution behavior of semiflexible linear polymers may be well described by the Kratky–Porod wormlike chain model [7, 8]. This model is defined as an elastic wire with bending energy in a thermal bath or a continuous limit of the freely rotating chain. Its chain stiffness is measured by the stiffness parameter λ^{-1}, which is equal to twice of the persistence length q (Note that, in general, $\lambda^{-1} \geq 2q$ and the equality holds in the case of the wormlike chain) [8]. The dimensional properties of the wormlike chain become functions of the reduced contour length λL ($\propto M$), where L is the contour length of the wormlike chain, the limits of $\lambda L \to 0$ and $\lambda L \to \infty$ corresponding to the rigid rod and random coil limits, respectively [8]. The wormlike chain becomes longer and more flexible (or shorter and stiffer) with increasing (or decreasing) λL. For analysis of the dilute solution behavior of semiflexible ring polymers, a ring version of the wormlike chain model, i.e., the wormlike ring model, then seems appropriate.

The wormlike ring model may be constructed from the linear wormlike chain (of contour length L and stiffness parameter λ^{-1}) by connecting its chain ends in such a way that the unit tangent vectors at both the ends coincide with each other. In the limit of $\lambda L \to 0$ and $\lambda L \to \infty$, the wormlike ring so constructed becomes the rigid ring of radius $L/2\pi$ and the random-coil (Gaussian) ring, respectively. Yamakawa and coworkers have calculated the mean-square radius of gyration $\langle S^2 \rangle$ [8, 9, 10], intrinsic viscosity $[\eta]$ [8, 9], and translational diffusion coefficient D [8, 9] for the wormlike ring model and proposed the interpolation formulas for these properties, although the application of the interpolation formulas for $[\eta]$ and D is limited to the range of large λL. Unfortunately, however, the existing wormlike ring theory is valid only for the *phantom* rings, i.e., the rings without the topological constraints, which work to preserve the type of knots of a given ring polymer.

For a deeper understanding of the dilute solution behavior of semiflexible rings, we have made theoretical and/or Monte Carlo (MC) studies of the second virial coefficient $A_{2,\Theta}$ at the Θ state [11, 12], which reflects the topological interaction between a pair of unlinked rings and then is positive even for ring polymers at the Θ state (without excluded volume effects) [13–17], and scattering function $P(k)$ with k the magnitude of scattering vector **k** [18, 19] by the use of the wormlike ring model. And also, we have examined effects of the topological constraints on $\langle S^2 \rangle$ [11–19], $[\eta]$ [20], $P(k)$ [18, 19], and $A_{2,\Theta}$ [11] by comparing the MC results for the phantom wormlike ring with those for the wormlike ring of the trivial or trefoil knot. In this review, these results are briefly summarized.

* Corresponding author.
E-mail address: ida@molsci.polym.kyoto-u.ac.jp.

https://doi.org/10.1016/j.reactfunctpolym.2018.06.007
Received 9 January 2018; Received in revised form 1 May 2018; Accepted 15 June 2018
Available online 20 June 2018
1381-5148/

2. Monte Carlo model—Discrete wormlike ring

In this section, we give a brief description of a discrete version of the wormlike ring model for MC simulations proposed by Frank-Kamenetskii et al. [8, 10, 21]. The discrete wormlike ring is composed of n junction points connected by n infinitely thin bonds of length l. Let $\mathbf{l}_i$ ($i = 1, 2, \cdots, n-1$) be the ith bond vector from the ith point to the ($i + 1$)th. The nth bond vector $\mathbf{l}_n$ completes the ring, i.e., $\sum_{i=1}^{n} \mathbf{l}_i = \mathbf{0}$. The configuration of the ring may then be specified by the set $\{\mathbf{l}_n\} = [\mathbf{l}_1, \mathbf{l}_2, \cdots, \mathbf{l}_{n-1}(, \mathbf{l}_n)]$ apart from its position and orientation in an external Cartesian coordinate system. Note that $\mathbf{l}_n$ is a dependent variable for the ring. The configurational energy U of the ring may be written in terms of the angle θ_i ($i = 2, 3, \cdots, n$) between $\mathbf{l}_{i-1}$ and $\mathbf{l}_i$ and θ_1 between $\mathbf{l}_n$ and $\mathbf{l}_1$ as follows,

$$U\left(\{\mathbf{l}_n\}\right) = \frac{\alpha}{2}\sum_{i=1}^{n}\theta_i{}^2, \tag{1}$$

where α is the bending force constant. The stiffness parameter λ^{-1} of the ring may be given by

$$\lambda^{-1} = l\frac{1 + \langle\cos\theta\rangle}{1 - \langle\cos\theta\rangle}, \tag{2}$$

where $\langle\cos\theta\rangle$ is defined by

$$\langle\cos\theta\rangle = \frac{\int_0^{\pi} e^{-\alpha\theta^2/2k_{\mathrm{B}}T}\cos\theta\sin\theta d\theta}{\int_0^{\pi} e^{-\alpha\theta^2/2k_{\mathrm{B}}T}\sin\theta d\theta} \tag{3}$$

with k_B the Boltzmann constant and T the absolute temperature. The discrete wormlike ring so defined becomes identical with the continuous wormlike ring of contour length L and of stiffness parameter λ^{-1} in the limit of $n \to \infty$ under the conditions of Eq. (2) with Eq. (3) and of $nl = L$ [10, 21]. Note that the discrete wormlike ring reduces to the freely jointed ring in the limit of $\alpha \to 0$. We adopt an n-sided regular polygon of side length l as the initial configuration and sequentially generate configurations without consideration of the topological constraints by the use of the Deutsch procedure [22], where a given configuration is deformed by rotating the shorter part of the ring around the vector connecting two junction points (not next to each other) randomly chosen by an angle randomly chosen in [π, π), along with the Metropolis method of importance sampling [23]. An ensemble so obtained is a mixture of configurations of all kinds of knots with the Boltzmann weight of U. This ensemble corresponds to the phantom wormlike ring.

Following the procedure of Vologodskii et al. [24] and of ten Brinke and Hadziioannou [25] to distinguish the trivial or trefoil knot from the others by the use of the Alexander polynomials [26, 27], we extract configurations of the trivial or trefoil knot from the mixture of configurations of all kinds of knots, and then, construct ensembles of configurations only of the trivial or trefoil knot. We note that the procedure on the basis of the Alexander polynomials cannot distinguish between the trivial knot and, e.g., the Kinoshita–Terasaka knot having 11 crossings [28], and also, between the trefoil knot and, e.g., the 8_{19} knot. However, effects of such complex knots may be regarded as negligibly small, if any, in the range of n and α/k_BT (or λ^{-1}) investigated.

By the use of the two or three kinds of ensembles, we calculated the MC values of $\langle S^2\rangle$, $[\eta]$, $P(k)$, and $A_{2,\Theta}$ in the ranges of $10 \le n \le 1000$ and $0 \le \alpha/k_BT \le 100$. These ranges of n and α/k_BT correspond to the range of $0.05 \lesssim \lambda L \le 1000$. Hereafter, all lengths are measured in units of λ^{-1} unless otherwise noted, for simplicity, so that, for example, λL is replaced by (reduced) L.

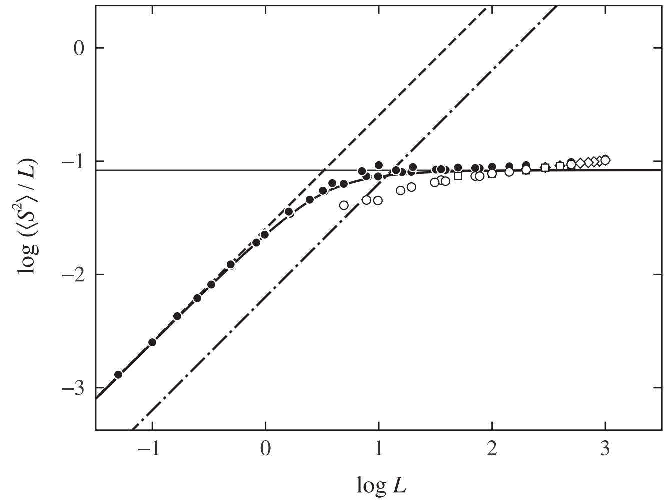

Fig. 1. Double-logarithmic plots of $\langle S^2\rangle/L$ against L for the phantom wormlike ring (solid curve), wormlike ring of the trivial knot (filled circles), and that of the trefoil knot (unfilled circles). The solid horizontal line segment represents the random-coil limiting value for the phantom ring. The dashed and dot-dashed straight line segments represent the theoretical values for the rigid ring of radius $L/2\pi$ and for the two rings of radius $L/4\pi$ overlapping with each other, respectively. The square and diamond represent the values for the freely jointed ring of the trefoil knot obtained by Dobay et al. [29] and by Moore et al. [30], respectively.

3. Mean-Square radius of gyration

In this section, we show the behavior of $\langle S^2\rangle$ as a function of L for the phantom wormlike ring and the wormlike ring of the trivial or trefoil knot.

Fig. 1 shows double-logarithmic plots of $\langle S^2\rangle/L$ against L for the wormlike rings. The solid curve represents the theoretical values of the (continuous) phantom wormlike ring calculated from the following interpolation formula proposed by Shimada and Yamakawa [8, 10].

$$\begin{aligned}\langle S^2\rangle &= \frac{L^2}{4\pi^2}\Big[1-0.1140L-0.0055258L^2 \\ &\quad + 0.0022471L^3-0.00013155L^4\Big] \quad \text{for } L < 6 \\ &= \frac{L}{12}\left(1-\frac{7}{6L}-0.025e^{-0.01L^2}\right) \quad \text{for } L \ge 6.\end{aligned} \tag{4}$$

The filled and unfilled circles represent the MC values for the wormlike ring of the trivial knots and of the trefoil knot, respectively. The square and diamond represent the values for the freely jointed ring of the trefoil knot obtained by Dobay et al. [29] and by Moore et al. [30], respectively. We note that Dobay et al. adopted the procedure for extracting configurations of the trefoil knot on the basis of the HOMFLY polynomials [26] and Moore et al. did the procedure proposed by Deguchi and Tsurusaki [31, 32] using not only the Alexander polynomials but also the Vassiliev invariants [33] of degree 2 and 3.

The theoretical values of the phantom wormlike ring (solid curve) first increase along the dashed straight line segment of slope unity, which represents the theoretical values of the rigid ring ($\langle S^2\rangle = L^2/4\pi^2$), then deviate downward, and finally approach the random-coil limiting value ($\langle S^2\rangle = L/12$ [1, 34, 35]) represented by the thin solid horizontal line segment, with increasing L. The MC values for the wormlike ring of the trivial knot (filled circles) almost agree with the values for the phantom wormlike ring for $L \lesssim 10$ (Strictly speaking, the MC data are somewhat scattered because of the discreteness of the MC model) and become larger progressively than the latter values for $L \gtrsim 10$ with increasing L. The MC data for the wormlike and freely jointed ring of the trefoil knot (unfilled circles, square, and diamond) form a single composite curve. The curve seems to first increase along the dot-dashed